

A global diagnostic of interior ocean ventilation

Bruno Blanke and Sabrina Speich

Laboratoire de Physique des Océans, Brest, France

Gurvan Madec

Laboratoire d'Océanographie Dynamique et de Climatologie, Paris, France

Rudy Maugé

Laboratoire de Physique des Océans, Brest, France

Received 3 July 2001; revised 30 August 2001; accepted 19 September 2001; published 30 April 2002.

[1] Ventilation is the process by which water is transferred from the surface mixed layer to the interior ocean. Ventilation anomalies as the result of climate variability may impact the atmosphere in remote regions where the flow returns to the mixed layer. From the Lagrangian analysis of monthly-mean ocean fields of a numerical model constrained by observed climatologies, we show that 324 Sv of mixed layer water travel throughout the interior ocean for periods longer than 12 months, leading to an average volume replacement time of roughly 125 yr. We evaluate the connections established on a global scale, with an appropriate mapping of the ventilation and corresponding obduction regions, and highlight the role of the Antarctic Circumpolar Current as a main receptacle of the water masses formed throughout the world ocean. *INDEX TERMS*: 4532 Oceanography: Physical: General circulation; 4283 Oceanography: General: Water masses; 1635 Global Change: Oceans (4203)

1. Introduction

[2] Water mass properties set by ocean–atmosphere interactions are carried away within the interior ocean by the ocean circulation. Depending on the underlying dynamics, the pathways for these newly-formed water masses may restrict to the subtropical and equatorial thermocline [Gu and Philander, 1997; Liu et al., 1994] or extend to interocean mass transfers [Gordon, 1986; Rintoul, 1991; Speich et al., 2001].

[3] Ventilation is the process by which water is transferred from the surface mixed layer to the interior ocean. It usually occurs over large scale domains as subduction [Luyten et al., 1983] or through much more localized convection areas [Semtner, 1976; Broecker et al., 1999]. As time scales usually proposed for ocean advection match the decadal period of various ocean-atmosphere feedbacks [Latif and Barnett, 1994], ocean-atmosphere interactions may control remotely further changes in atmospheric climate variability, by means of anomalies being advected within the interior ocean [Gu and Philander, 1997].

[4] Ventilation achieved by subduction [Luyten et al., 1983] is usually diagnosed with hydrographic data or model results related to a late winter mixed layer, calculating the annual-mean advective export of water at its bottom [Stommel, 1979; Marshall et al., 1993; Williams et al., 1995]. Ventilation achieved by convection [Semtner, 1976; Broecker et al., 1999] is related to severe atmospheric conditions (as surface cooling, sea-ice formation or enhanced evaporation) and may occur over longer periods [Mauritzen and Häkkinen, 1997].

[5] We investigate in this study the ventilation rate of the global ocean by a Lagrangian analysis of a numerical simulation strongly

constrained on observed climatologies for both temperature and salinity.

2. Method

[6] Multiple 3D trajectory calculations [Speich et al., 2001; Döös, 1995; Blanke et al., 1999, 2001] are computed from the monthly archive of velocity and tracer fields of the OPA model [Madec et al., 1998], run in a global, non eddy-resolving mode. The resolution is 2° in the zonal direction, with a meridional grid interval varying from 0.5° at the equator to a maximum of 1.9° in the tropic, and 31 levels in the vertical with the highest resolution (10 m) in the upper 150 meters. The bottom topography and the coastlines are derived from a global atlas [Smith and Sandwell, 1997] completed by values from the 5' × 5' ETOPO5 dataset. The model is forced by mean seasonal atmospheric fluxes, obtained from the ECMWF 15-year (1979–1993) reanalyses and smoothed by a 11-day running mean, and its density field is strongly constrained on an observational dataset of temperature and salinity [Levitus, 1982].

[7] The model offers a discrete representation (with successive monthly-mean states) of the time-varying surface mixed layer. Therefore, the mass flux escaping this layer is described in two complementary ways: we document with particles the advective mass transfer to the interior ocean during each month of the climatological year, and we also describe the flux transferred to the interior ocean on the occasion of abrupt (monthly) shallownings of the surface mixed layer [Cushman-Roisin, 1987]. The total number of particles we use is over several million as any of them explains only a fraction of the total transport, not to exceed a prescribed maximum value (here 10⁻³Sv per documented month, 1 Sv = 10⁶ m³/s) [Döös, 1995; Blanke and Raynaud, 1997]. As mass is conserved in the ocean model and as the Lagrangian trajectory scheme respects this constraint, all the particles injected into the thermocline return to the mixed layer, without intercepting coastlines or topography, or being trapped in the interior ocean.

[8] The exact volume of detained surface water depends on the criterion used for the definition of the surface mixed layer. For this global simulation, we adopt a uniform definition related to a maximum density difference of 0.01 m³/s between the surface and the last model level within the mixed layer. Then, to concentrate on genuine interior ocean ventilation, we eliminate from further diagnostics particles with journeys shorter than one year, since they explain only mass injection limited to the seasonal thermocline.

3. Results

3.1. Time and Density Binning

[9] The intensity of the remaining flow is poorly sensitive to the initial definition of the surface mixed layer. We decompose it into annual bins covering the full range of the advective journeys.

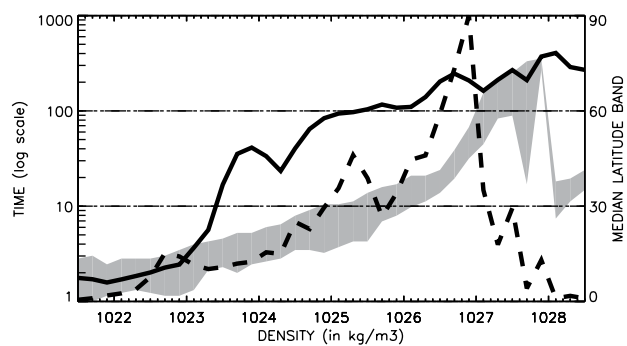


Figure 1. Mean renewal time scales in years (solid line, left-hand axis) as a function of surface density (in kg/m^3), with corresponding median bands of longitude (shaded area, right-hand axis) and ventilation fluxes (dashed line, arbitrary unit).

[10] The signal decreases with time, as longer periods correspond to a larger dispersion of the particles. The particles travelling for more than 1 yr explain 324 Sv: this is our estimate for the ventilation rate of the global interior ocean, 60% of which being achieved over periods shorter than 10 yr, and 22% inside the 10–100 yr window. An average residence time can be derived as the ratio of the interior ocean global volume to the ventilation rate and comes close to 125 years. It may be compared to the average residence time for fresh water in the oceans within Earth's hydrological cycle (roughly 4000 years) [Open University, 1997]. Therefore, ocean internal dynamics proves very efficient in mixing surface and interior waters.

[11] We derive more selective replacement time scales by analyzing water masses properties at the exact time they leave the surface mixed layer, averaging the travel times of particles referring to equivalent (0.2 kg/m^3) initial density classes (Figure 1). Corresponding ventilation fluxes and median bands of latitude accounting for half of them are also given. Tropical light waters (with density lower than 1024.0 kg/m^3) present short renewal time scales of the order of 1 to 40 yr, in agreement with a shallow position of the upper thermocline and active equatorial upwelling processes. Subducting subtropical waters (1024.7 to 1028.7 kg/m^3) are related to longer scales (up to a hundred years). Modal and intermediate waters (1026.5 to 1027.1 kg/m^3), formed mostly in the Southern Ocean and in the Northeastern Atlantic, take an active part in ventilation, with mean time scales that exceed 250 yr. Denser water masses characteristic of deep (Arctic) or bottom (Antarctic) water formation have the longest renewal time

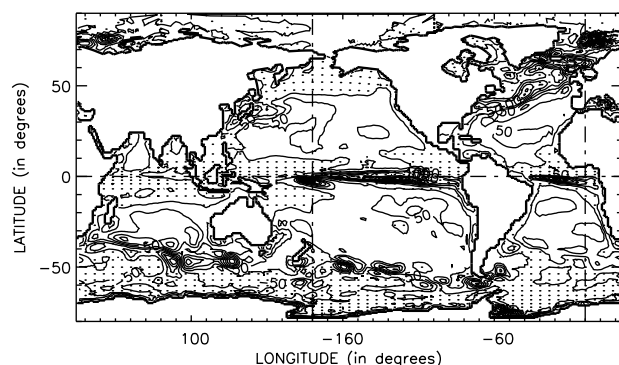


Figure 2. Net ventilation rate for the global ocean contoured with a 50 m/yr contour interval, as diagnosed from the initial and final positions of the trajectories documenting the ventilation process. Dotted areas refer to movements from the interior ocean to the surface mixed layer.

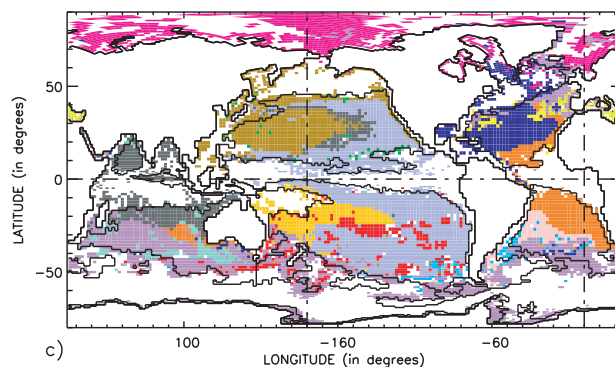
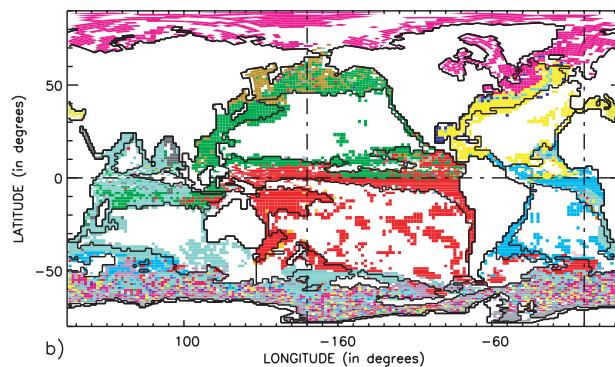
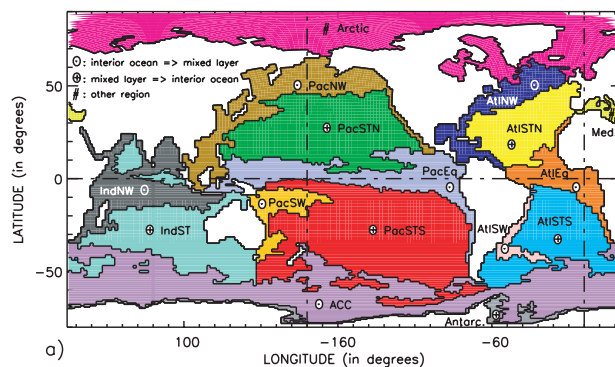


Figure 3. (a) Partitioning of the global ocean into 16 regions related to dominant mass transfers from (respectively to) the surface mixed layer, to (respectively from) the interior ocean (except for the Mediterranean Sea and the Arctic domain where mixed processes occur). (b) Color mapping of water mass origins over model gridcells linked to a transfer of interior ocean water to the surface mixed layer. (c) Color mapping of water mass fates over model gridcells linked to a transfer of surface mixed layer water to the interior ocean (ventilation).

scales, but never exceeding 400 years, in agreement with modeling views of the overturning circulation [Weaver *et al.*, 1993].

3.2. The Global Ventilation Field

[12] Figure 2 proposes a global mapping for the net ventilation rate. It is obtained by summing algebraically each infinitesimal positive (respectively negative) transport at the initial (respectively final) particle's location over the relevant model horizontal gridcell, and normalizing the result by each gridcell area. We find some net ventilation south of 70°S , associated with bottom water formation in the neighborhood of the Weddell and Ross Seas. The southern portion of the Antarctica Circumpolar Current (ACC) is dominantly associated with a return flow from the

Table 1. Mass Transfers (in Sv) Through Interior Ocean Ventilation Between Pairs of Regions Defined in Figure 3a

	Arctic	Med.	AtlSTN	AtlSTS	PacSTN	PacSTS	IndST	Antarc.	Other	Total
Arctic	12.0	0.0	1.0	0.0	0.0	0.0	0.0	0.0	0.5	13.5
Med.	0.0	1.5	0.5	0.0	0.0	0.0	0.0	0.0	0.0	2.0
AtlNW	4.5	0.5	16.5	1.5	0.0	1.0	2.5	0.0	3.0	29.5
AtlEq	0.5	0.0	3.5	13.0	0.0	0.5	5.0	0.0	0.5	23.0
AtlSW	0.0	0.0	0.0	5.5	0.0	0.5	0.0	0.0	0.5	6.5
PacNW	0.0	0.0	0.0	0.0	20.0	1.0	0.5	0.0	6.5	28.0
PacEq	0.0	0.0	0.0	0.5	15.0	39.5	2.0	0.0	3.5	60.5
PacSW	0.0	0.0	0.0	0.0	0.0	9.5	0.0	0.0	0.5	10.0
IndNW	0.0	0.0	0.0	0.0	7.0	1.5	12.0	0.0	3.0	23.5
ACC	8.0	1.0	4.0	10.0	1.0	14.0	30.5	9.0	13.5	90.0
Other	0.5	0.5	2.0	3.5	2.5	9.5	14.0	0.0	5.0	37.5
Total	25.0	3.5	27.5	34.0	45.0	77.0	66.5	9.0	36.5	324.0

permanent thermocline to the mixed layer (obduction), which is consistent with a locally divergent surface circulation. The mid-latitude band extending from 50°S exhibits an obvious inclination for subduction processes, as a direct response to wind forcing and associated downward Ekman pumping. The eastern coastal and equatorial rails reveal upwelling phenomena, bringing subsurface water into the mixed layer. The intense ventilation visible in the southwest equatorial Pacific is linked to a local distribution of mass within the equatorial thermocline, and may be attributed to the use of a too strict criterion on density for an optimal definition of the equatorial mixed layer. The north equatorial and subtropical basins (from 10°N to 40°N) present subduction behaviors similar to that of their southern counterparts, and ventilation rates match published estimates fairly well with values locally exceeding 50 or even 150 m/yr [Marshall *et al.*, 1993; Williams *et al.*, 1995]. The return flow into the mixed layer at mid-latitudes occurs essentially along the western and subpolar edges of the subtropical gyres [Qiu and Huang, 1995]. Deep water formation in the Arctic Sea, north of 60°N, is characterized by net mass injection in the interior ocean.

3.3. Mass Transfers from and to the Interior Ocean

[13] We quantify mass transfers to and from the interior ocean by coloring 16 convenient regions (see color code on Figure 3a). Each of which is associated preferentially with water mass formation or obduction. The Lagrangian framework allows the calculation of mass transfers between any of these regions with an accuracy better than 0.5 Sv, as listed for selected pairs in Table 1, summing the infinitesimal transport of the particles achieving the same connection. Using their initial and final positions as well as the code proposed in Figure 3a, we give a selective mapping of preferred destinations over the gridcells where occurs ventilation (Figure 3b). An equivalent view (Figure 3c) is proposed for water mass origins mapped over the gridcells where there is obduction. Let us focus on two rewarding examples. We diagnose first the origins of upwelled water within the equatorial and eastern coastal Atlantic (23 Sv). A dominant fraction is formed within the southern subtropical gyre (light blue areas in Figure 3b, 13 Sv). The northern subtropical gyre contributes up to 3.5 Sv (yellow) whereas 21% of the upwelling (the area along Africa) is made of waters collected from the Indian subtropical gyre (5 Sv, pale green). Then we may investigate the fates of the waters formed in the subtropical North Pacific (Figure 3c). The innermost area (light brownish, 20 Sv) evidences connections achieved with the Kuroshio region in the Northwest Pacific. The most external area (light blue, 15 Sv) shows connections with the equatorial Pacific. Grey areas (7 Sv) link the subtropical Pacific to the tropical Indian Ocean through Indonesia.

[14] Water mass formation occurs dominantly in the Pacific Ocean (134 Sv), whereas the Indian and Atlantic Oceans contribute equally (70.5 and 72 Sv, respectively). Though internal connections restricted to the ACC, the Arctic, Atlantic, Indian or Pacific Oceans account for almost two thirds of the global ventilation, the ACC

mixed layer collects more than 35% of the waters formed within the global ocean, the largest fraction of which coming from remote basins.

4. Conclusion

[15] Our global quantification and our picture of interior ocean ventilation are obtained by means of an ocean model forced by seasonal atmospheric fluxes and constrained on observed climatologies for temperature and salinity [Levitus, 1982], and acting as a dynamical interpolator. These constraints force a large-scale circulation (mostly geostrophic in the interior ocean) that forms a solid basis for subsequent large-scale Lagrangian diagnostics. Our results emphasize the connections achieved throughout the interior ocean by ventilation, proposing quantitative estimates for transports and renewal time scales. Further diagnostics are needed to determine the detailed structure of the internal pathways, and to assess the full sensitivity of these estimates to the definition chosen for the mixed layer vertical extent, to the uncertainties of the surface and internal constraints applied to the ocean model and to the presence of mesoscale features not sampled in the current framework.

[16] **Acknowledgments.** This work was supported by grants from the European Community (TRACMASS project, contract MAS3-CT97/0142) and the French Centre National de la Recherche Scientifique (Action Thématique Innovante from the Institut National des Sciences de l'Univers).

References

- Blanke, B., and S. Raynaud, Kinematics of the Pacific Equatorial Undercurrent: a Eulerian and Lagrangian approach from GCM results, *J. Phys. Oceanogr.*, 27, 1038–1053, 1997.
- Blanke, B., M. Arhan, G. Madec, and S. Roche, Warm water paths in the equatorial Atlantic as diagnosed with a general circulation model, *J. Phys. Oceanogr.*, 29, 2753–2768, 1999.
- Blanke, B., S. Speich, G. Madec, and K. Döös, A global diagnostic of interocean mass transfers, *J. Phys. Oceanogr.*, 31, 1623–1632, 2001.
- Broecker, W. S., S. Sutherland, and T.-H. Peng, A possible 20th-century slowdown of Southern Ocean deep water formation, *Science*, 286, 1132–1135, 1999.
- Cushman-Roisin, B., Dynamics of the Oceanic Surface Mixed Layer, in Proceedings Hawaiian Winter Workshop, edited by P. Muller and D. Henderson, pp. 181–196, Hawaii Inst. Of Geophysics Special Publications, 1987.
- Döös, K., Interocean exchange of water masses, *J. Geophys. Res.*, 100, 13,499–13,514, 1995.
- Gordon, A. L., Interocean exchange of thermocline water, *J. Geophys. Res.*, 91, 5037–5046, 1986.
- Gu, D., and S. G. H. Philander, Interdecadal climate fluctuations that depend on exchanges between the tropics and extratropics, *Science*, 275, 805–807, 1997.
- Latif, M., and T. P. Barnett, Causes of decadal climate variability over the north Pacific and north America, *Science*, 266, 634–637, 1994.
- Levitus, S., Climatological Atlas of the World Ocean, *NOAA Prof. Paper* 13, 173 pp., U. S. Govt. Printing Office, 1982.

- Liu, Z., S. G. H. Philander, and R. C. Pacanoswki, A GCM study of tropical-subtropical upper-ocean water exchange, *J. Phys. Oceanogr.*, *24*, 2606–2623, 1994.
- Luyten, J. R., J. Pedlosky, and H. Stommel, The ventilated thermocline, *J. Phys. Oceanogr.*, *13*, 292–309, 1983.
- Madec, G., P. Delecluse, M. Imbard, and C. Lévy, OPA 8.1 Ocean General Circulation Model reference manual, *Notes du Pôle de Modélisation de l'Institut Pierre-Simon Laplace II*, 91, 1998.
- Marshall, J. C., A. J. G. Nurser, and R. G. Williams, Inferring the subduction rate and period over the North Atlantic, *J. Phys. Oceanogr.*, *23*, 1315–1329, 1993.
- Mauritzen, C., and S. Häkkinen, Influence of sea ice on the thermohaline circulation in the Arctic-North Atlantic Ocean, *Geophys. Res. Lett.*, *24*, 3257–3260, 1997.
- Open University Course Team Sea water: Its composition, properties and behaviour, 168 pp., Butterworth-Heinemann Editors, 1997.
- Qiu, B., and R. X. Huang, Ventilation of the North Atlantic and North Pacific: Subduction versus obduction, *J. Phys. Oceanogr.*, *25*, 2374–2390, 1995.
- Rintoul, S. R., South Atlantic interbasin exchange, *J. Geophys. Res.*, *96*, 2675–2692, 1991.
- Semtner, A. J., Jr., Numerical simulation of the Arctic Ocean circulation, *J. Phys. Oceanogr.*, *6*, 409–425, 1976.
- Smith, W. H. F., and D. T. Sandwell, Global sea floor topography from satellite altimetry and ship depth sounding, *Science*, *277*, 1956–1962, 1997.
- Speich, S., B. Blanke, and G. Madec, Warm and cold water paths of a GCM thermohaline conveyor belt, *Geophys. Res. Lett.*, *28*, 311–314, 2001.
- Stommel, H., Determination of water mass properties of water pumped down from the Ekman layer to the geostrophic flow below, *Proc. Natl. Acad. Sci. U.S.A.*, *76*, 3051–3055, 1979.
- Weaver, A. J., J. Marotzke, P. F. Cummins, and E. S. Sarachik, Stability and variability of the thermohaline circulation, *J. Phys. Oceanogr.*, *23*, 39–60, 1993.
- Williams, R. G., M. A. Spall, and J. C. Marshall, Does Stommel's mixed-layer "demon" work?, *J. Phys. Oceanogr.*, *25*, 3089–3102, 1995.

B. Blanke, S. Speich, and R. Mauge, Laboratoire de Physique des Océans, UFR Sciences et Techniques, 6 av. Le Gorgeu - BP809, 29285 Brest CEDEX, France. (blanke@univ-brest.fr; speich@univ-brest.fr; rmauge@univ-brest.fr)

G. Madec, Laboratoire d'Océanographie Dynamique et de Climatologie, Université Pierre et Marie Curie - Case 100, 4 Place Jussieu, 75252 Paris CEDEX 05, France. (gm@lodyc.jussieu.fr)